# Local theory of the slanted homoclinic snaking bifurcation diagram

U. Bortolozzo,[1] M. G. Clerc,[2] and S. Residori[1]
[1]*INLN, Université de Nice Sophia-Antipolis, CNRS, 1361 route des Lucioles 06560 Valbonne, France*
[2]*Departamento de Física, Facultad de Ciencias Físicas y Matemáticas, Universidad de Chile, Casilla 487-3, Santiago, Chile*

Localized states in out of equilibrium one-dimensional systems are described by the homoclinic snaking associated with the infinite sequence of multibump localized solutions of the corresponding time reversible dynamical system. We show that when the pattern undergoes a saddle-node bifurcation the homoclinic snaking bifurcation diagram becomes slanted and a finite set of localized states continue to exist outside the region of bistability. This generic behavior offers a local theory resolution of the discrepancy between models and experiments.

Pattern formation in out of equilibrium dynamical systems leads sometimes to the appearance of localized states, that is, the pattern extends over a limited space region and consists of only a few cells, eventually one, of the corresponding extended structure. Examples are numerous, such as oscillons in vibrated granular media [1] and in vibrated fluids [2], filaments of current in plasmas [3], spots in chemical reactions [4] and in vegetation patterns [5], magnetic domains in computer memories [6], cavity solitons in semiconductor microcavities [7], localized optical structures in atomic vapors [8], and in liquid crystals experiments [9,10]. The large number of experimental observations has inspired many theoretical works on the origin of localized states. Starting from the pioneering work of Woods and Champneys [11], developed models are based on the one-dimensional description of the time reversible dynamical system associated to a generalized Swift-Hohenberg equation. In this framework, localized states are understood as the homoclinic orbits originating from a homogeneous stationary state and passing close to the periodic orbit associated to a pattern state, generating an infinite sequence of limit points, at each point the homoclinic orbit creating another bump. Hence, the bifurcation diagram of the homoclinic displays a snaking shape [11]. An extension of the above scenario has been given in Ref. [12] and, more recently, the same dynamical evolution have been presented in terms of front interaction [13]. All these models are based on the coexistence of two states, namely, a stable homogeneous state and a stable pattern.

Despite the ability of these theoretical approaches to give an intuitive picture of the phenomenon, the comparison with the experiments remains up to now hard to establish, even from a qualitative point of view. The main discrepancy originates from the large robustness of the one-bump solution, often existing outside the bistability region that is required by the theory, and from the lack of a clear observation of the multibump solutions expected from the snaking sequence. A tentative resolution to the theory-experiment discrepancy has recently been proposed, which resorts to the addition of a nonlocal nonlinearity in the Swift-Hohenberg model, leading to a tilt of the snaking bifurcation diagram [14,15]. However, even though nonlocality could be justified for some systems, for many experiments there is no direct evidence or demonstration that nonlocality should indeed exist or play a relevant role, and, in any case, introducing a global coupling implies a strong modification of the physical context into which the theoretical models are developed.

Here, we present a local theory of the slanted homoclinic snaking and we show that tilting the snaking bifurcation diagram does not need to invoke an extra mechanism, such as global coupling or nonlocal nonlinearity, but can generically result from a modification of the phase portrait associated to the time-reversible dynamical system as it was considered in the original theoretical framework [11,12]. As an example, we consider a generic Ginzburg-Landau model including a spatial forcing and bistability between an homogeneous and a pattern state, and we allow the pattern to lose its stability through a saddle-node bifurcation. We show that the saddle node of the pattern tilts the homoclinic snaking and thus destroys the infinite sequence of homoclinic orbits associated to the multibump localized structures. As a consequence, only the single-bump solution, or a few of these states, remain, which are robust localized structures living outside the bistability region once the pattern has disappeared. This example, that provides an alternative resolution of the discrepancy between theory and experiments, does not need a large perturbation of the original theory but is instead a quite natural extension of it, insofar it simply includes the possibility, not considered before, that the pattern may lose its stability for some parameter ranges.

We thus consider a model which has a tunable coexistence region between a uniform state and a pattern, the real sub-sub-critical Ginzburg-Landau equation with spatial forcing

$$\partial_t A = \varepsilon A + \nu|A|^2 A - \alpha|A|^4 A + |A|^6 A + \partial_{xx} A + \eta A^2 e^{iqx}, \quad (1)$$

where $A(x,t)$ is a complex amplitude, $\varepsilon$ is the bifurcation parameter, $\{\nu,\alpha\}$ control the type of the bifurcation (first or second order depending on the sign of these coefficients), $\eta$ is the amplitude, and $q$ the wave number of the spatial forcing. This extra term accounts for the nonadiabatic effect and restores the original discrete symmetry of the pattern solution [16]. The above model describes simultaneously a primary and a secondary subcritical spatial bifurcation of a homogeneous state and a pattern state, respectively. While the unforced amplitude equation $\eta=0$ has been widely used to explain pattern formation in dissipative systems [17], the forced equation $\eta\neq 0$ has been used to describe traveling

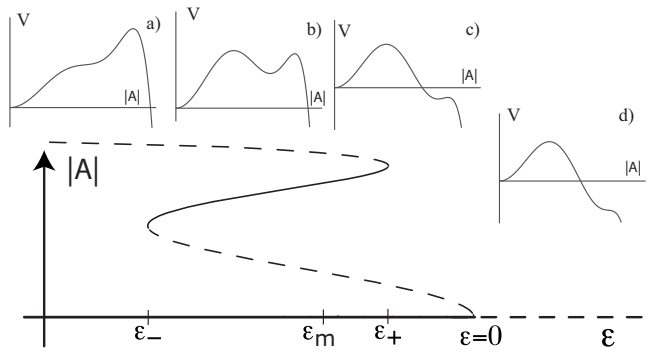


FIG. 1. Bifurcation diagram of the unforced model (1), $\eta=0$. The insets represent the potential as a function of $|A|$ in different regions of the bifurcation diagram: (a) close to the left-side saddle node $\varepsilon_-$, (b) just before the Maxwell point $\varepsilon_m$, (c) after the Maxwell point, (d) close to the right-side saddle node $\varepsilon_+$. The solid and dashed curves represent the stable and the unstable states, respectively.

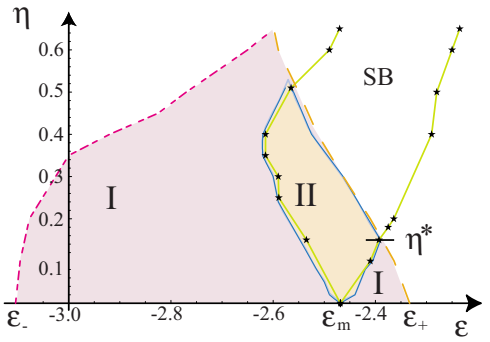


FIG. 2. (Color online) Phase diagram of the model (1) calculated for $\nu=7.0$, $\alpha=4.9$, and $q=12$. The whole bistability region extends over areas I and II while the pinning range is region II. The dashed, dotted (red) curves represent the saddle-node bifurcation of the stable pattern with the large, respectively, small amplitude unstable pattern. The smallest localized structure, that is, the single-bump solution, is observed inside the solid (green) open curve and, after the saddle node, continues to exist in the SB region.

waves in convection [16], localized patterns [13], localized peaks [18], localized structures in monoatomic layer deposition [19], and noise-induced front propagation [20,21].

The unforced amplitude equation is variational, i.e.,

$$\partial_t A = -\frac{\delta \mathcal{F}}{\delta \bar{A}}, \tag{2}$$

where the functional

$$\mathcal{F} \equiv \int V(|A|) + (\partial_x A)^2 dx,$$

$V \equiv -\varepsilon|A|^2 - \nu|A|^4/2 + \alpha|A|^6/3 - |A|^8/4$ is the potential, and the dynamics is characterized by the relaxation of the functional $\mathcal{F}$. For some positive values of $\nu$, $\alpha$ and negative value of $\varepsilon$, the system exhibits coexistence between two stable homogeneous states, a zero ($A=0$) and a nonzero ($A\neq 0$) uniform amplitude state. Figure 1 shows the typical bifurcation diagram as a function of the bifurcation parameter $\varepsilon$ and the respective potentials in different regions of the diagram. There is a particular value of $\varepsilon=\varepsilon_m$—Maxwell point—where a front solution connecting the two homogeneous states is motionless, that is, the two states have the same potential value ($V=0$). For $\varepsilon<\varepsilon_m$ ($\varepsilon>\varepsilon_m$) the zero (nonzero) amplitude state invades the nonzero (zero) uniform state. When $\varepsilon$ is increased or decreased with respect to the Maxwell point, the nonzero uniform state disappears by saddle-node bifurcation, that is, this stable state merges with the unstable uniform one. These bifurcation points are represented by $\varepsilon_-$ and $\varepsilon_+$ in Fig. 1. The inset figures represent the potential (a) close to the left-side saddle node, (b) just before the Maxwell point, (c) after the Maxwell point, and (d) close to the right-side saddle node. Notice that by changing $\{\alpha,\nu\}$, one can tune the range of the coexistence region.

Including the nonlinear spatial forcing $\eta\neq 0$ modifies the previous scenario in the following way. The zero uniform state remains a solution. However, the nonzero uniform state becomes a spatial periodic state, with wave number $q$ and amplitude proportional to $\eta$ and oscillating around the nonzero state of the unforced system. Hence, the system now exhibits coexistence between a stable homogeneous state and a stable pattern state. In the same way as for the unforced model, the bifurcation diagram as a function of $\varepsilon$ presents a coexistence region, now between an homogenous state and a pattern, whereas the two unstable branches correspond to two unstable patterns with different amplitudes. Thus, by changing the bifurcation parameter $\varepsilon$ the stable pattern disappears by a saddle-node bifurcation either with the large amplitude ($\varepsilon_+$) or with the small amplitude pattern ($\varepsilon_-$).

The simulation software DimX developed at INLN has been used for numerical simulations. Figure 2 illustrates the numerically calculated phase diagram of the above model in the $\{\eta,\varepsilon\}$ plane. The area I plus area II is the zone of bistability between the pattern and the homogeneous state. The dashed, dotted curves represent the saddle-node bifurcation of the stable pattern with the unstable pattern with large, respectively, small amplitude. The region II is the pinning range, where a front connecting the uniform state with the pattern is motionless [22]. Around this region, one expects that the system exhibits a family of localized patterns, which are the multibump solutions resulting from the heteroclinic tangle of repulsive and attractive manifolds of the homogeneous and the pattern state [11–13]. This heteroclinic tangle generates an infinite number of homoclinic curves, each homocline representing one of the multibump solutions. The corresponding bifurcation diagram has a complex structure and is termed homoclinic snaking bifurcation [11].

For small $\eta$, inside the pinning range, numerical calculations of the homoclinic snaking bifurcations give a typical diagram, as the one shown in Fig. 3(a) for $\eta=0.1$. However, when $\eta$ is increased beyond a critical value $\eta^*$ in the $\{\eta,\varepsilon\}$ plane, the saddle-node line of patterns collapses with the pinning range and, as a consequence of the pattern disappearance, the homoclinic tangle changes drastically. Numerical calculations lead to a slanted homoclinic snaking bifurcation diagram, as the one reported in Fig. 3(b) for $\eta=0.4$. Hence, when $\eta>\eta^*$, the homoclinic snaking becomes slanted, that is, the model (1) exhibits a finite set of multibump solutions

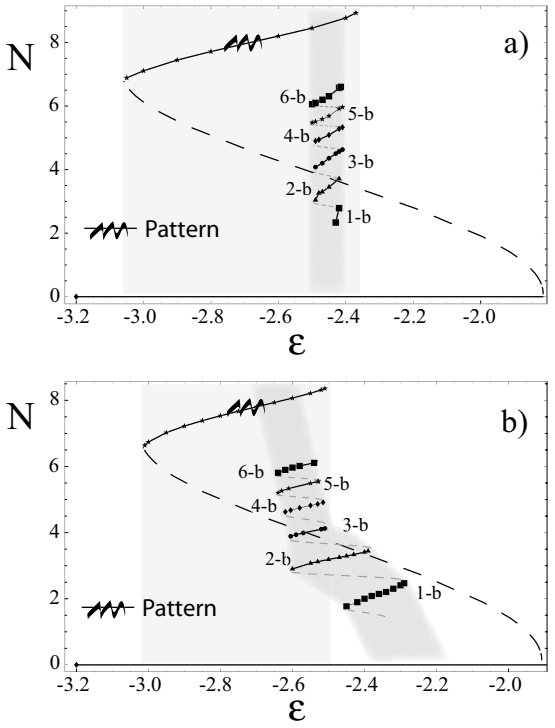


FIG. 3. Homoclinic snaking bifurcation of model (1) calculated for (a) $\eta$=0.1 and (b) $\eta$=0.4. The horizontal axis is the bifurcation parameter $\varepsilon$ and the vertical axis is the norm ($\mathcal{N}$), where $\mathcal{N}=\sqrt{\int \mathrm{Re}(A)^2+\mathrm{Im}(A)^2 dx}$. The solid, dashed curves stand, respectively, for the stable, unstable state. The single-bump, double-bump, and so forth, solutions are depicted by the solid lines 1-b, 2-b, etc. Points are the results of the numerical calculations.

outside the coexistence region. Eventually, when $\eta$ is increased only the single-bump localized structure persists in a large region of the parameter space. Numerically, we observe that the attraction basin of two-bump, three-bump, and so forth solutions becomes, respectively, smaller and smaller. Indeed, when the homoclinic snaking is tilted, it also shrinks for solutions with a large number of bumps whereas it stretches for solutions with a small number of bumps [see Fig. 3(b)]. Outside the bistability region and for large $\eta$, the model (1) exhibits single-bump localized states, that is, only the smallest size localized pattern is observed. This region of parameter is denoted as the zone single bump (SB) in Fig. 2. Numerically, we verify that when we perturb the uniform state in this region, a set of uncorrelated single spots appear instead of a correlated pattern.

Slanted snaking bifurcations also occur for localized peaks appearing over a patterned background. Experimentally, localized peaks are observed in liquid crystal optical systems [10,18] and in vertically driven fluids [2]. Numerically, localized peaks have been predicted in monoatomic layer deposition [23] and in optical cavity containing a Kerr and a photonic crystal [24]. As for the localized structures over a homogeneous state, the robust observation is that localized peaks are single bump. In an analogous way as for localized structures, we can explain this robust phenomenon as a consequence of the saddle-node bifurcation of one pattern state. We thus consider a model that exhibits two ingredients: coexistence between two spatially periodic states and a tunable saddle-node bifurcation. This is a variant of Eq. (1), where the sign of the highest nonlinear term is inverted, i.e.,

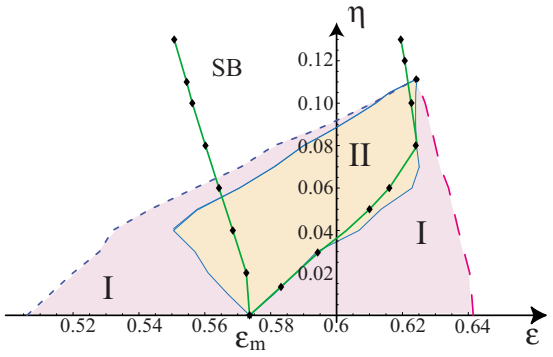


FIG. 4. (Color online) Phase diagram of the model (3) calculated for $\nu$=2.43, $\alpha$=2.87, and $q$=12. The whole bistability region extends over areas I and II while the pinning range is region II. The dashed, dotted (red) curves represent the saddle-node bifurcation of the stable pattern with the large, respectively, small amplitude unstable pattern. The smallest localized peak, that is, the single-bump solution, is observed inside the solid (green) open curve and, after the saddle node, continues to exist in the SB region.

$$\partial_t A = \varepsilon A + \nu|A|^2 A - \alpha|A|^4 A - |A|^6 A + \partial_{xx} A + \eta A^2 e^{iqx}. \quad (3)$$

For negative $\nu$, $\alpha$, and $\eta \neq 0$, the bifurcation diagram of the above model is characterized by a primary supercritical spatial bifurcation followed by a secondary subcritical spatial bifurcation. Thus, for some values of parameters, the system exhibits coexistence between two pattern states whose amplitudes are proportional to $\eta$. Figure 4 depicts the phase diagram in the $\{\eta, \varepsilon\}$ plane, where the same notation as in Fig. 2 has been used.

Similar to the model (1), for small intensity of the forcing $\eta$, the stationary dynamical system of model (3) exhibits a heteroclinic tangle. Thus, the system presents a family of multibump localized solutions appearing over a patterned background. Numerically, we obtain the bifurcation diagram of these solutions, which is the typical snaking bifurcation located inside the pinning range (region II of Fig. 4). However, when the forcing is increased—after the saddle node of the pattern—the homoclinic snaking starts to incline and becomes similar to that shown in Fig. 3(b). This leads to single-bump localized peaks existing in a large area of parameters outside the bistability region (region SB of Fig. 4), in qualitative agreement with the experimental observations [18].

In conclusion, we have shown a local theory of the slanted homoclinic snaking, which results from a saddle-node bifurcation of the pattern state. As a consequence, we have shown that localized states can exist without bistability and that single-bump localized structures are, in general, the most robust solutions. These results agree with the numerous observations of localized structures in such different fields as granular media, magnetic materials, optics, fluids, chemistry, vegetation, where a nonlocal theory is not always justified,

thus providing an alternative, and general, resolution of the discrepancy between models and experiments. Moreover, similar homoclinic snaking bifurcation scenarios are expected to occur with other types of bifurcations of the pattern state. Work in this direction is in progress.

M.G.C. acknowledges the financial support from the ring program ACT15 of *Programa Bicentenario de Ciencia y Tegnología* of the Chilean government and FONDAP Grant No. 11980002. This work has been partially supported by Grant No. ANR-07-BLAN-0246-03 *turbonde*.

[1] P. B. Umbanhowar, F. Melo, and H. L. Swinney, Nature (London) **382**, 793 (1996).
[2] H. Arbell and J. Fineberg, Phys. Rev. Lett. **85**, 756 (2000).
[3] Y. A. Astrov and Y. A. Logvin, Phys. Rev. Lett. **79**, 2983 (1997).
[4] K-Jin Lee, W. D. McCormick, J. E. Pearson, and H. L. Swinney, Nature (London) **369**, 215 (1994).
[5] J. von Hardenberg, E. Meron, M. Shachak, and Y. Zarmi, Phys. Rev. Lett. **87**, 198101 (2001).
[6] Th. O'Dell, Rep. Prog. Phys. **49**, 589 (1986).
[7] S. Barland *et al.*, Nature (London) **419**, 699 (2002).
[8] B. Schäpers, M. Feldmann, T. Ackemann, and W. Lange, Phys. Rev. Lett. **85**, 748 (2000).
[9] P. L. Ramazza, E. Benkler, U. Bortolozzo, S. Boccaletti, S. Ducci, and F. T. Arecchi, Phys. Rev. E **65**, 066204 (2002).
[10] U. Bortolozzo, R. Rojas, and S. Residori, Phys. Rev. E **72**, 045201(R) (2005).
[11] P. D. Woods and A. R. Champneys, Physica D **129**, 147 (1999).
[12] P. Coullet, C. Riera, and C. Tresser, Phys. Rev. Lett. **84**, 3069 (2000).
[13] M. G. Clerc and C. Falcon, Physica A **356**, 48 (2005).
[14] W. J. Firth, L. Columbo, and A. J. Scroggie, Phys. Rev. Lett. **99**, 104503 (2007).
[15] J. H. P. Dawes, SIAM J. Appl. Dyn. Syst. **7**, 186 (2008).
[16] D. Bensimon, B. I. Shraiman, and V. Croquette, Phys. Rev. A **38**, 5461 (1988).
[17] G. Nicolis and I. Prigogine, *Self-Organization in Nonequilibrium Systems: From Dissipative Structures to Order Through Fluctuations* (Wiley, New York, 1977).
[18] U. Bortolozzo, M. G. Clerc, C. Falcon, S. Residori, and R. Rojas, Phys. Rev. Lett. **96**, 214501 (2006).
[19] M. G. Clerc, E. Tirapegui, and M. Trejo, Phys. Rev. Lett. **97**, 176102 (2006).
[20] M. G. Clerc, C. Falcon, and E. Tirapegui, Phys. Rev. Lett. **94**, 148302 (2005); Phys. Rev. E **74**, 011303 (2006).
[21] M. G. Clerc, D. Escaff, C. Falcon, and E. Tirapegui, Eur. Phys. J. Spec. Top. **143**, 171 (2007).
[22] Y. Pomeau, Physica D **23**, 3 (1986).
[23] M. G. Clerc, E. Tirapegui, and M. Trejo, Eur. Phys. J. Spec. Top. **146**, 407 (2007).
[24] D. Gomila and G. L. Oppo, Phys. Rev. A **76**, 043823 (2007).